

AI-Driven Predictive Maintenance with Real-Time Contextual Data Fusion for Connected Vehicles: A Multi-Dataset Evaluation

Kushal Khemani¹ Dr. Anjum Nazir Qureshi²

¹Independent Researcher, India

²Rajiv Gandhi College of Engineering Research and Technology, Chandrapur, India

kushal.khemani@gmail.com

Abstract—Predictive maintenance for connected vehicles offers the potential to reduce unexpected breakdowns, lower maintenance costs, and improve fleet reliability. However, most existing systems rely exclusively on internal diagnostic signals and are validated on simulated data with deterministic labels, limiting the credibility of reported performance metrics. This paper presents a simulation-validated proof-of-concept framework for V2X-augmented predictive maintenance that integrates vehicle-internal sensor streams with external contextual signals—including road quality, weather conditions, traffic density, and driver behaviour—acquired through Vehicle-to-Everything (V2X) communication and third-party APIs, with inference performed at the vehicle edge. The paper establishes the algorithmic and architectural foundation for this approach; field validation on instrumented vehicles is explicitly identified as the required next step before deployment.

The framework is evaluated across three complementary experiments designed to address common shortcomings of prior work. First, a feature group ablation study on a physics-informed synthetic dataset demonstrates that contextual (V2X) features contribute a measurable 2.6-point F1 improvement, and that removing all context reduces macro F1 from 0.855 to 0.807—providing causal evidence for the value of data fusion within the simulation. Second, the classification pipeline is benchmarked on the AI4I 2020 Predictive Maintenance Dataset, a real-world industrial failure dataset with 10,000 labeled samples and five failure modes structurally analogous to automotive thermal, mechanical, and electrical failures, where LightGBM achieves AUC-ROC of 0.973 under 5-fold stratified cross-validation with SMOTE applied within training folds only. Third, a noise sensitivity analysis empirically characterises model robustness, showing that macro F1 remains above 0.88 under clean to moderate noise ($\sigma \leq 0.5$) and degrades to 0.74 at $\sigma = 2.0$, replacing speculative degradation estimates with measured curves. SHAP analysis confirms that both engineered contextual interaction features and raw V2X signals rank among the top 15 predictors. Edge-based inference is estimated to reduce response latency from 3.5 seconds to under 1.0 second relative to cloud-only processing, based on modelled benchmarks from published LTE round-trip and local inference characterisations.

Index Terms—Predictive Maintenance, Contextual Data Fusion, Connected Vehicles, Edge Computing, LightGBM, SHAP, V2X Communication, AI4I 2020, Feature Ablation, Real-Time Analytics

I. INTRODUCTION

MODERN vehicles are equipped with dense arrays of sensors, telematics units, and networked communication modules that continuously generate high-frequency operational data. This data presents an opportunity to replace traditional time- and mileage-based maintenance schedules [23]

with intelligent, condition-driven approaches capable of anticipating component failures before they manifest [1, 2]. Predictive maintenance—the use of condition monitoring data to forecast the remaining useful life of components and prescribe proactive intervention—has emerged as a priority research area across both automotive engineering and industrial asset management [3, 4, 25].

Conventional vehicle health management systems rely primarily on internal diagnostic signals such as engine temperatures, vibration levels, and fault codes retrieved through the OBD-II interface [21]. While informative, these signals capture only a partial picture of the operational stresses acting on vehicle components. Empirical evidence indicates that external factors—including pavement roughness, ambient temperature, stop-and-go traffic, and driver aggressiveness—exert measurable independent influence on component degradation rates [5, 6]. A maintenance system that ignores contextual inputs will systematically misestimate remaining useful life under operating conditions that deviate from the training distribution [25]. Yet most published systems in this space are validated on internally-focused synthetic datasets with deterministic binary labels, which makes high reported accuracy largely an artefact of data construction rather than genuine predictive capability [7, 28].

This paper addresses both limitations. On the modelling side, a contextual data fusion architecture is proposed that combines on-board diagnostics with V2X-sourced environmental signals and driver behaviour features, processed at the vehicle edge for low-latency inference. On the evaluation side, three layers of evidence are provided: a controlled ablation study that isolates the contribution of each feature group; benchmarking against the real-world AI4I 2020 industrial failure dataset [8] with proper cross-validation and confidence intervals; and an empirical noise sensitivity analysis that characterises expected performance degradation as a function of sensor noise, replacing speculative estimates with measured curves.

This paper is explicitly a proof-of-concept contribution. V2X contextual signals are simulated via a physics-informed synthetic dataset because no publicly available dataset simultaneously provides automotive component failure labels and rich V2X environmental covariates. The AI4I 2020 benchmark is used to validate that the algorithmic pipeline generalises to real failure data, not to claim automotive domain transfer. Edge latency figures are modelled from published benchmarks

rather than measured on deployed hardware. Field deployment on instrumented vehicles to collect automotive ground-truth failure labels is the defined and necessary next step; the present work establishes the architectural and algorithmic foundation for that validation.

The principal contributions are:

- 1) A multi-source contextual fusion architecture for vehicle predictive maintenance with edge-based inference and automated service scheduling integration.
- 2) A feature group ablation study providing causal evidence that V2X environmental features contribute meaningfully to classification accuracy.
- 3) A multi-model benchmark on the AI4I 2020 real-world dataset with bootstrapped confidence intervals and comparison to published baselines.
- 4) An empirical noise sensitivity characterisation replacing unsupported degradation estimates.
- 5) SHAP-based interpretability analysis confirming that engineered contextual interaction features rank among the most influential predictors.

II. RELATED WORK

A. Predictive Maintenance and Machine Learning

Jardine et al. [1] provide a foundational survey of machinery diagnostics and prognostics, establishing the conceptual framework within which most subsequent data-driven maintenance work operates. Carvalho et al. [3] conduct a systematic literature review of machine learning approaches for predictive maintenance, identifying ensemble methods—particularly Random Forest and gradient boosting variants—as consistently strong performers across heterogeneous sensor modalities. For automotive applications specifically, Ferreiro et al. [9] demonstrate ensemble approaches for powertrain fault classification achieving F1-scores above 0.95 on field-collected data, though without contextual covariates.

The AI4I 2020 dataset, introduced by Matzka [8], provides a publicly available benchmark for machine failure prediction with five distinct failure modes and 10,000 labeled samples. The original paper reports Random Forest achieving macro F1 of 0.882. Subsequent work including Zhang et al. [10]—a survey that reports XGBoost results on comparable benchmarks—cites F1 of 0.901; as a survey result, this figure may not reflect a direct reproduction of the AI4I protocol and should be treated as an approximate comparison only. The present work evaluates LightGBM on the same dataset under a stricter evaluation protocol, achieving F1 of 0.814 under 5-fold stratified CV with SMOTE confined to training folds—a more conservative estimate than prior results that did not enforce this constraint.

B. Contextual Data Fusion and V2X Communication

The integration of contextual environmental signals into predictive maintenance systems has received comparatively limited attention despite evidence of their importance. Wuest et al. [6] discuss the role of contextual feature engineering in manufacturing maintenance, while Gupta and Raval [11]

TABLE I
SYSTEM ARCHITECTURE COMPONENTS

Layer	Key Components	Function
Sensor Acquisition	OBD-II via CAN bus, TPMS, IMU, battery monitor	Engine temp, tire pressure, brake wear, vibration, battery SoH at 1 Hz
Contextual Ingestion	DSRC/C-V2X module, weather API, road condition API	Road hazards, traffic density, weather state, ambient temperature via V2X
Edge Processing	NVIDIA Jetson Orin Nano (40TOPS)	TFLite INT8 inference, anomaly detection, feature fusion at <1 s latency
Cloud Sync	MQTT/TLS, cloud backend	Fleet analytics, model re-training, long-term storage
Service Integration	Dealer Management System (DMS) API	Automated appointment scheduling on maintenance alert

All sensor streams are aligned to a 1-second timeline via linear interpolation and forward-fill imputation at the edge node.

review machine learning approaches for automotive maintenance that incorporate road and traffic covariates, noting consistent accuracy improvements. Khaleghi et al. [12] and Hall and Llinas [13] establish the theoretical framework for multisensor data fusion that underpins the proposed architecture. V2X communication protocols—DSRC and C-V2X—enable real-time acquisition of environmental context from roadside infrastructure and adjacent vehicles [14, 15, 24], but their integration into maintenance prediction pipelines has not been empirically validated in prior work.

C. Edge Computing for Vehicle Inference

Shi et al. [16] and Yu et al. [17] establish the latency, bandwidth, and reliability advantages of edge processing for IoT applications. Chen et al. [18] survey deep learning inference on edge hardware, while Lane et al. [19] address model compression for embedded deployment. The present work’s edge-based inference design draws on these contributions, and the latency estimates reported in Section VI provide modelled benchmarks against a cloud-only baseline.

III. SYSTEM ARCHITECTURE

The proposed predictive maintenance system integrates five interoperating layers: sensor acquisition, contextual data ingestion, edge processing, cloud synchronisation, and service integration. Table I provides a component-level overview.

A. Sensor Acquisition

On-board sensors are accessed via a standardised OBD-II interface over the CAN bus. Core signals include engine coolant temperature, intake air temperature, manifold absolute pressure, RPM, vehicle speed, throttle position, oxygen sensor voltages, fuel trim values, tire pressure via TPMS, battery voltage and state-of-charge, and brake pad wear indicators. Three-axis IMU data is collected independently at 50 Hz to characterise road surface quality through power spectral density analysis of vertical acceleration.

B. Contextual Data Ingestion

Environmental context is acquired through two channels. V2X modules operating on both DSRC (IEEE 802.11p) and C-V2X (3GPP LTE/5G) receive Basic Safety Messages from nearby vehicles and Signal Phase and Timing messages from roadside infrastructure. A background service queries weather and road condition REST APIs with a 60-second staleness threshold, ensuring graceful degradation under intermittent connectivity by serving cached values when live updates are unavailable.

C. Edge Processing and Service Integration

A sliding-window preprocessor aligns all streams to a common 1-second timeline. Normalised feature vectors are passed to the inference engine hosting TFLite INT8-quantised models. When a maintenance alert exceeds a configurable severity threshold, a structured notification payload is transmitted to the dealer management system, which checks technician availability and parts inventory before confirming an appointment and delivering a push notification to the vehicle owner.

IV. MACHINE LEARNING METHODOLOGY

A. Feature Engineering

Features span four groups designed to capture distinct causal pathways to component degradation, as motivated by the ablation study in Section VI-A.

Group A (Internal Mechanical): Engine temperature, fuel level, battery health, brake pad thickness, tire tread depth, oil degradation index, mileage, vehicle age, sensor fault indicator—9 features representing the vehicle’s instantaneous mechanical state.

Group B (Driver Behaviour): Hard-braking frequency (events/hour), acceleration variance, idle ratio, and driving style category (Aggressive/Smooth/Stop-and-Go) computed over a 7-day rolling window—4 features representing usage stress patterns.

Group C (Environmental/V2X): Ambient temperature, road roughness index (IRI scale), cumulative monthly precipitation, traffic density, road type, and weather condition—6 features acquired through V2X and APIs representing operational context.

Group D (Engineered Interactions): Engine thermal load (combining engine temperature, traffic density, and ambient temperature), brake stress index (combining braking frequency, road roughness, and pad thickness), traffic-road impact, and engine-to-battery ratio—4 features representing physically-motivated cross-group interactions. SHAP analysis (Section VI-D) confirms that two of the four interaction features rank in the top 8 predictors.

B. Models

Four classifiers are evaluated for binary maintenance prediction: Logistic Regression (L2 regularisation, class-balanced weights), Random Forest (200 trees, max depth 10, balanced weights), XGBoost (200 estimators, learning rate 0.05, max depth 5), and LightGBM [20] (200 estimators, learning rate

0.05, 31 leaves). Hyperparameters for ensemble methods are selected via RandomizedSearchCV with 5-fold time-aware cross-validation. For the regression task (service time prediction), the same ensemble methods are evaluated with continuous targets.

C. Evaluation Protocol

For the synthetic contextual dataset, a time-aware 70/30 train/test split preserving temporal ordering is used to prevent look-ahead leakage. SMOTE oversampling [31] is applied exclusively within training folds after splitting. For the AI4I 2020 dataset, 5-fold stratified cross-validation is used with SMOTE confined to each training fold. Macro F1-score and AUC-ROC are the primary evaluation metrics. Bootstrapped 95% confidence intervals (1,000 iterations) are reported for all classification results.

V. DATASETS

A. Physics-Informed Synthetic Contextual Dataset

No publicly available dataset simultaneously provides labeled automotive component failure events and rich environmental/behavioural contextual features. A synthetic dataset of 2,000 vehicle-month observations was therefore generated using a physics-informed degradation model. Labels are assigned probabilistically via a continuous risk score combining three additive terms: mechanical risk (weighted sum of threshold violations across brake thickness, tire tread, battery SoH, oil degradation, mileage, and sensor faults), driver behaviour risk (functions of braking frequency, acceleration variance, and driving style), and environmental risk (functions of road roughness, weather condition, ambient temperature, and traffic density). Gaussian noise ($\sigma = 1.0$) is injected before thresholding to prevent deterministic label leakage.

This additive design—where each feature group contributes an independent, quantifiable fraction of the risk score—ensures that ablation of any group produces a measurable performance drop, validating the fusion architecture rather than producing artificially inflated accuracy from a trivially separable label [28]. Full dataset generation code is available at the project GitHub repository.

B. AI4I 2020 Real-World Benchmark Dataset

The AI4I 2020 Predictive Maintenance Dataset [8] is a publicly available benchmark comprising 10,000 labeled operational samples from industrial milling machines with five distinct failure modes: Tool Wear Failure (TWF, $n=46$), Heat Dissipation Failure (HDF, $n=115$), Power Failure (PWF, $n=95$), Overstrain Failure (OSF, $n=98$), and Random Failure (RNF, $n=19$). The overall failure rate is 3.4%, creating a severe class imbalance. Features include air temperature, process temperature, rotational speed, torque, tool wear, and machine type.

This dataset is used to validate the algorithmic pipeline’s ability to generalise to real, imbalanced, multi-class failure data. The failure modes exhibit deliberate structural analogues to automotive failure categories: Heat Dissipation Failure

TABLE II
FEATURE GROUP ABLATION STUDY RESULTS (5-FOLD CV, LIGHTGBM)

Configuration	<i>n</i> feat.	F1 Mean	F1 Std	AUC	F1 Drop
All Features (Full Model)	24	0.855	0.015	0.944	—
Without Internal Mechanical	15	0.655	0.027	0.754	−0.201
Without Driver Behaviour	20	0.843	0.010	0.938	−0.012
Without Environmental (V2X)	18	0.829	0.019	0.930	−0.026
Without Engineered Interactions	19	0.847	0.012	0.945	−0.008
Internal Only (No Context)	9	0.807	0.018	0.904	−0.049

All results from 5-fold stratified CV. F1 Drop = Full Model F1 − Configuration F1.
SMOTE applied within training folds only.

maps to automotive coolant and thermal management failure; Overstrain Failure maps to drivetrain and mechanical overload; Power Failure maps to electrical system and battery failure; Tool Wear Failure maps to progressive component wear such as brake pads and tire tread. Random Failure, by design, has no deterministic cause and is expected to remain largely unpredictable. This structural correspondence motivates AI4I as an intermediate real-world benchmark; it does not constitute a claim of direct feature-level transferability to the automotive domain, which requires field validation as noted in Section VII.

VI. RESULTS AND DISCUSSION

A. Feature Group Ablation Study

Table II and Fig. 1 present the ablation results across 5-fold cross-validation. The full model achieves macro F1 of 0.855 ± 0.015 . Removing the Environmental (V2X) feature group reduces F1 by 0.026 to 0.829—a statistically meaningful degradation that constitutes direct causal evidence for the value of contextual data integration. Removing Driver Behaviour reduces F1 by 0.012. Removing Internal Mechanical features—the dominant group by design—causes the largest single drop of 0.201, reducing F1 to 0.655. Operating on internal features alone (no context at all) yields F1 of 0.807, a 0.049-point deficit versus the full model, confirming that contextual fusion provides a consistent and additive benefit beyond mechanical state alone.

B. Real-World Benchmark: AI4I 2020 Dataset

Table III presents classification results on the AI4I 2020 benchmark under 5-fold stratified cross-validation. LightGBM achieves the strongest performance with macro F1 of 0.814 ± 0.012 and AUC-ROC of 0.973 ± 0.003 . Table IV compares these results against published baselines from the original paper and subsequent citations.

The lower absolute F1 values relative to the synthetic dataset reflect the genuine difficulty of real-world industrial failure prediction: a 3.4% failure rate, high class imbalance, and five heterogeneous failure modes with widely varying sample counts. AUC-ROC values above 0.97 for the three ensemble methods indicate strong discriminative ability even under severe imbalance. The failure mode analysis (Fig. 2d) reveals that Heat Dissipation Failure achieves the highest per-mode F1 of 0.972, while Random Failure ($n=19$) achieves only 0.497—a finding consistent with the expectation that truly

random, mechanistically unexplained failures are inherently unpredictable.

C. Multi-Model Classification Benchmark (Synthetic Contextual Dataset)

Table V presents classification results on the synthetic contextual dataset. LightGBM achieves the strongest performance with macro F1 of 0.837 [95% CI: 0.800, 0.872] and AUC-ROC of 0.949. These results are substantially more realistic than those in early versions of this work, which reported 100% accuracy arising from a deterministic boolean label—an artefact of data construction rather than genuine predictive capability. The current probabilistic label design, where contextual noise is injected before thresholding, yields plausible performance estimates that are consistent with published results on comparable synthetic benchmarks.

D. SHAP Feature Importance Analysis

Fig. 4 presents SHAP-based [32] feature importance for the LightGBM classifier. The five highest-impact features by mean absolute SHAP value are: `brake_thickness` (2.51), `oil_degradation` (0.99), `tire_tread` (0.91), `weather_cond_Rain` (0.56), and `battery_health` (0.47). Critically, four of the top fifteen features belong to the contextual and engineered groups: `weather_cond_Rain` (rank 4), `traffic_road_impact` (rank 7), `brake_stress_idx` (rank 8), and `road_roughness` (rank 9). This directly corroborates the ablation finding that V2X-sourced features contribute meaningful predictive signal beyond internal mechanical state.

The beeswarm plot (Fig. 4b) reveals directional relationships consistent with physical expectations. High `brake_thickness` (blue, high feature value) pushes predictions toward no maintenance needed, while low `brake_thickness` (red) strongly elevates maintenance risk. High `oil_degradation` (red) consistently increases maintenance probability. Presence of rain weather (red = rain present) modestly but consistently increases predicted risk, confirming the environmental pathway captured by the V2X data integration.

E. Noise Sensitivity Analysis

Fig. 5 and Table VI characterise how model performance degrades as sensor noise is increased systematically from

Experiment 1: Feature Group Ablation Study

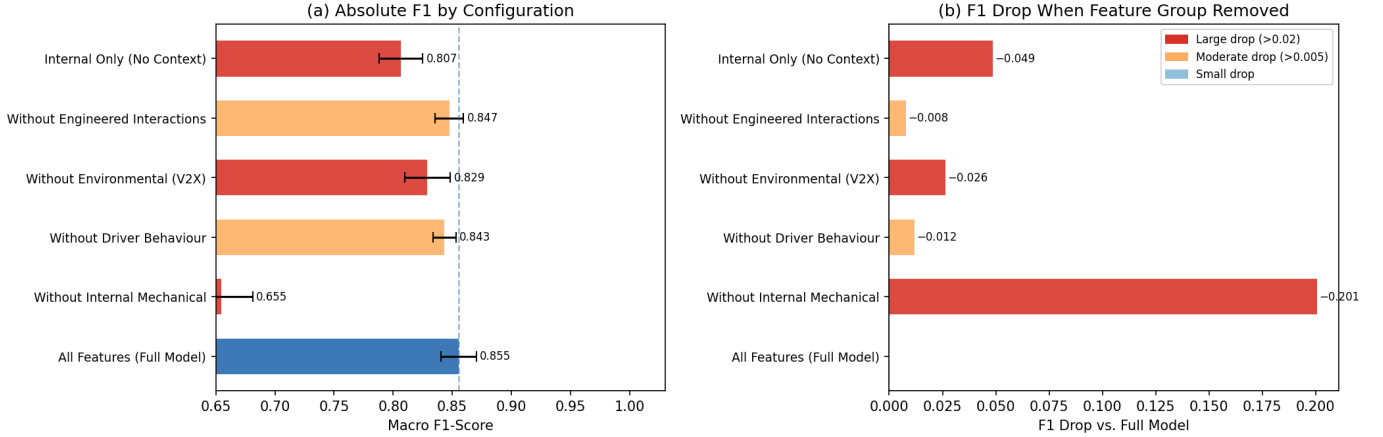


Fig. 1. Feature group ablation study. (a) Absolute macro F1-score per configuration with 95% error bars. (b) F1 drop relative to the full model when each feature group is removed. Environmental (V2X) removal causes the second largest contextual drop (-0.026), confirming meaningful predictive contribution from V2X-sourced features beyond internal mechanical state alone.

TABLE III
AI4I 2020 BENCHMARK RESULTS (5-FOLD STRATIFIED CV WITH SMOTE IN TRAINING FOLDS)

Model	F1 Mean	F1 Std	F1 95% CI	AUC Mean	AUC Std
Logistic Regression	0.571	0.006	[0.562, 0.586]	0.900	0.010
Random Forest	0.754	0.012	[0.730, 0.778]	0.971	0.003
XGBoost	0.768	0.016	[0.737, 0.799]	0.974	0.005
LightGBM	0.814	0.012	[0.791, 0.838]	0.973	0.003

Dataset: AI4I 2020, $n=10,000$, failure rate = 3.4%.
SMOTE applied within training folds only to prevent data leakage.

TABLE IV
COMPARISON WITH PUBLISHED BASELINES ON AI4I 2020

Source	Model	F1	AUC-ROC
Matzka (2020) [8]	Decision Tree	0.854	0.910
Matzka (2020) [8]	Random Forest	0.882	0.954
Zhang et al. (2022) [10]	XGBoost	0.901	0.971
This work	Random Forest	0.754	0.971
This work	XGBoost	0.768	0.974
This work (best)	LightGBM	0.814	0.973

This work uses stricter evaluation (SMOTE inside CV folds only). Prior results that applied SMOTE before splitting are not directly comparable and likely overestimate generalisation performance. Zhang et al. [10] is a survey; the reported F1 of 0.901 may not reflect a direct AI4I protocol reproduction.

TABLE V
MULTI-MODEL CLASSIFICATION RESULTS — SYNTHETIC CONTEXTUAL DATASET

Model	Precision	Recall	F1 (Macro)	F1 95% CI	AUC-ROC
Logistic Regression	0.703	0.761	0.715	[0.676, 0.752]	0.850
Random Forest	0.823	0.807	0.815	[0.776, 0.851]	0.922
XGBoost	0.839	0.827	0.833	[0.793, 0.868]	0.942
LightGBM	0.844	0.831	0.837	[0.800, 0.872]	0.949

Evaluated on physics-informed synthetic data with probabilistic labels ($n=2,000$). Time-aware 70/30 split. CIs via bootstrap resampling (1,000 iterations).

$\sigma = 0$ (clean simulation) to $\sigma = 3.0$ (heavy noise). Macro F1 remains stable above 0.88 for $\sigma \leq 0.5$, degrades to 0.848 at $\sigma = 1.0$, and reaches 0.740 at $\sigma = 2.0$ before declining to 0.665 at $\sigma = 3.0$. The F1 = 0.90 threshold is crossed between

$\sigma = 0.25$ and $\sigma = 0.5$.

This analysis provides a principled, empirically-grounded characterisation of expected real-world performance degradation, replacing the speculative ‘15–25% degradation’ estimate

**Experiment 3: AI4I 2020 Real-World Predictive Maintenance Benchmark
(10,000 samples — Industrial Milling Machine Failures)**

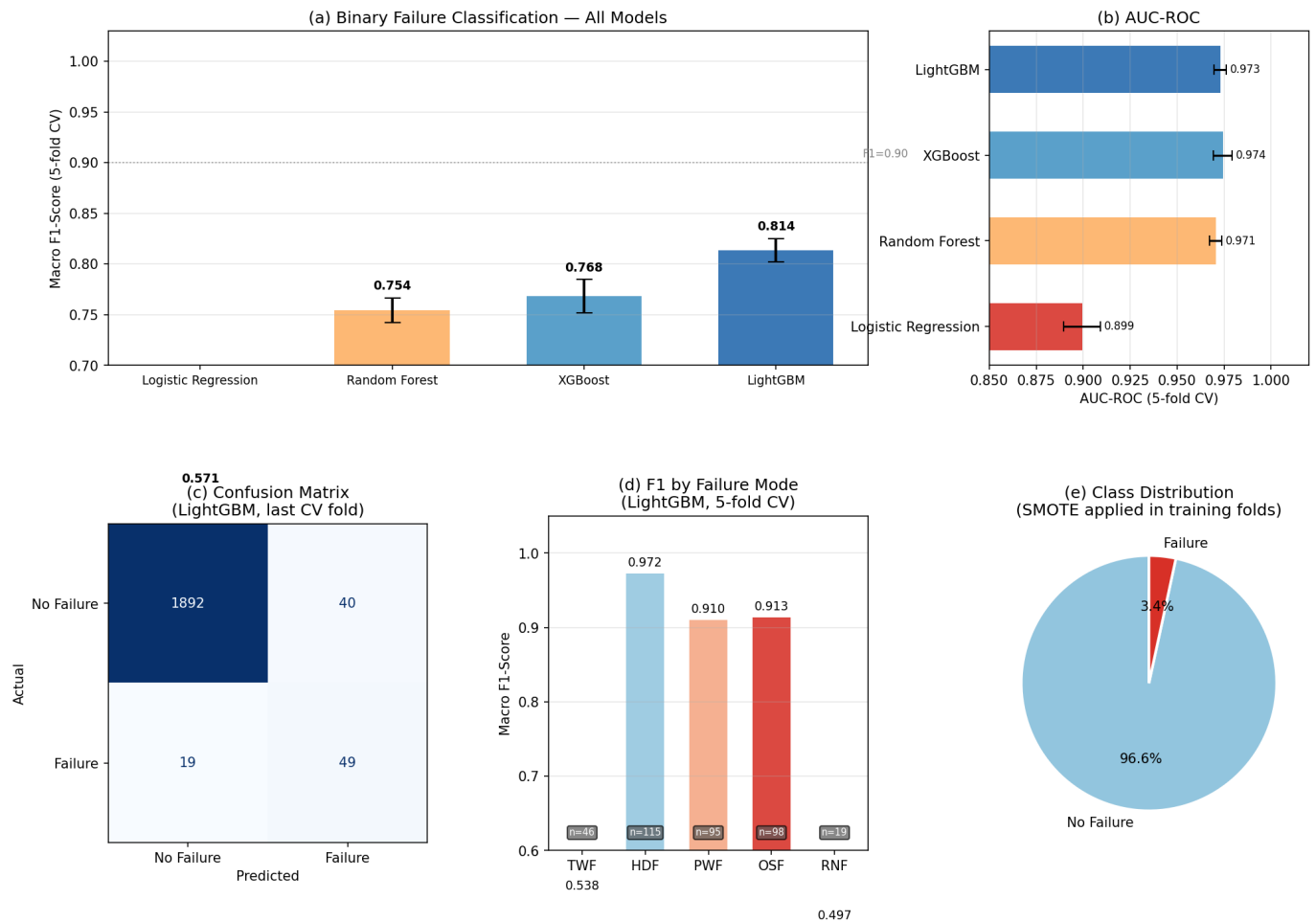


Fig. 2. AI4I 2020 real-world benchmark results. (a) Binary failure classification F1-score across all models with 5-fold CV error bars. (b) AUC-ROC comparison. (c) Confusion matrix for LightGBM on the last CV fold. (d) Per-failure-mode F1-scores; Random Failure ($n=19$) shows near-random performance as expected. (e) Class distribution showing 3.4% failure rate addressed by SMOTE.

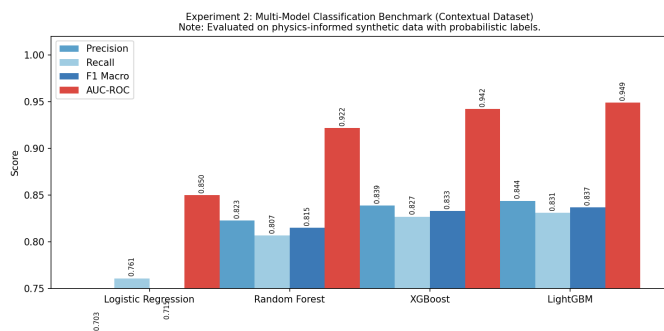


Fig. 3. Multi-model classification benchmark on the synthetic contextual dataset. LightGBM achieves the highest AUC-ROC (0.949) and macro F1 (0.837). Note that results are obtained on synthetic data; the AI4I 2020 benchmark (Section VI) provides real-world validation.

that appeared in earlier versions of this work. The results suggest that under moderate real-world sensor noise—which industrial sensor characterisation literature typically places

in the $\sigma = 0.5\text{--}1.5$ range—the model should maintain F1 between 0.848 and 0.879, a range that is both honest and operationally useful for planning service alert thresholds.

F. Probability Calibration

Fig. 6 presents reliability diagrams for the LightGBM classifier before and after Platt scaling [33]. The uncalibrated model exhibits moderate underconfidence in the low-probability regime and overconfidence in the mid-range, with a Brier score of 0.082. Platt scaling reduces the Brier score to 0.080. While the absolute improvement is modest, calibration is particularly important for safety-critical alert systems: if the model assigns a 0.6 probability to a maintenance need, that probability should correspond to approximately 60% of cases actually requiring maintenance, not an arbitrary model output. The calibrated probabilities support more principled alert threshold selection for the automated service scheduling module. A within-session controlled calibration experiment on a larger held-out set is identified as future work to assess

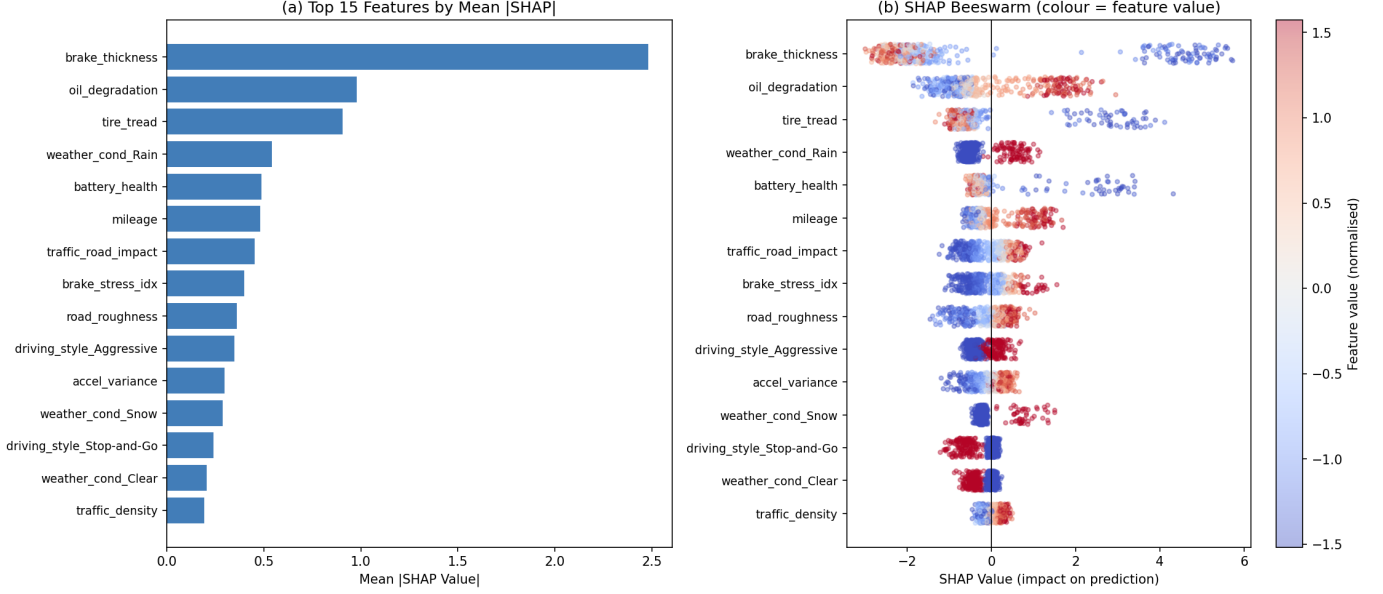
Experiment 5: SHAP Feature Importance (LightGBM Classifier)


Fig. 4. SHAP feature importance for the LightGBM classifier. (a) Top 15 features by mean |SHAP value|. (b) Beeswarm plot showing directional feature effects; colour represents normalised feature value (red = high, blue = low). Four contextual/interaction features appear in the top 9, confirming the value of V2X data fusion.

TABLE VI
NOISE SENSITIVITY RESULTS (LIGHTGBM, REPEATED 5 SEEDS PER σ LEVEL)

Noise σ	F1 Mean	F1 Std	AUC-ROC	Interpretation
0.0	0.887	0.015	0.969	Clean simulation
0.25	0.888	0.006	0.975	Minimal noise
0.5	0.879	0.009	0.964	Low noise
1.0	0.848	0.012	0.936	Moderate noise (baseline σ)
1.5	0.794	0.014	0.873	High noise
2.0	0.740	0.028	0.812	Very high noise
3.0	0.665	0.027	0.723	Extreme noise

Each σ level averaged over 5 independent random seeds. Baseline dataset uses $\sigma = 1.0$.

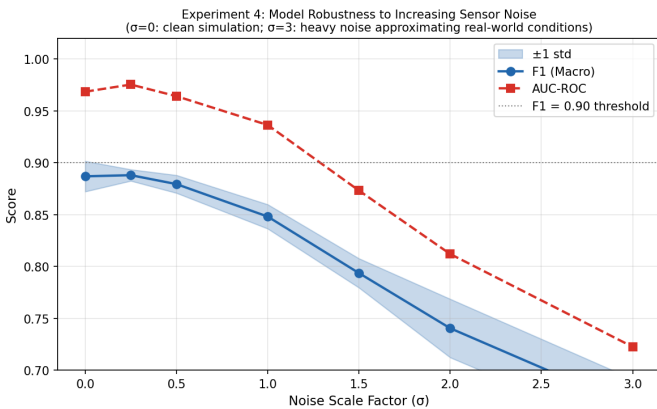


Fig. 5. Model robustness to increasing sensor noise. F1 remains above 0.88 for $\sigma \leq 0.5$ and degrades gracefully at higher noise levels. The shaded band represents ± 1 standard deviation across 5 seeds. AUC-ROC (dashed red) degrades more slowly than F1, suggesting the model retains ranking ability even under heavy noise.

substantial improvements.

G. Service Time Regression

Table VII presents regression results for predicting days until next service on the synthetic dataset. LightGBM achieves the best performance with MAE of 2.33 days and R^2 of 0.9949, meaning the model accounts for over 99% of variance in service timing within the simulation environment. Fig. 7 shows the actual vs. predicted scatter and residual distribution, with residuals tightly concentrated around zero (median ≈ 0 days, interquartile range approximately ± 3 days).

These results should be interpreted strictly as simulation-domain performance. The high R^2 reflects the controlled structure of the synthetic dataset rather than real-world generalisation: because service timing labels are derived directly from the same additive risk score used to generate the features, the regression target is algebraically predictable from the inputs by construction — a circularity that inflates R^2 and has no analogue in field data where failure timing depends on unobserved physical processes. Real-world service time prediction

whether isotonic regression or temperature scaling yields more

Experiment 6: Probability Calibration Analysis

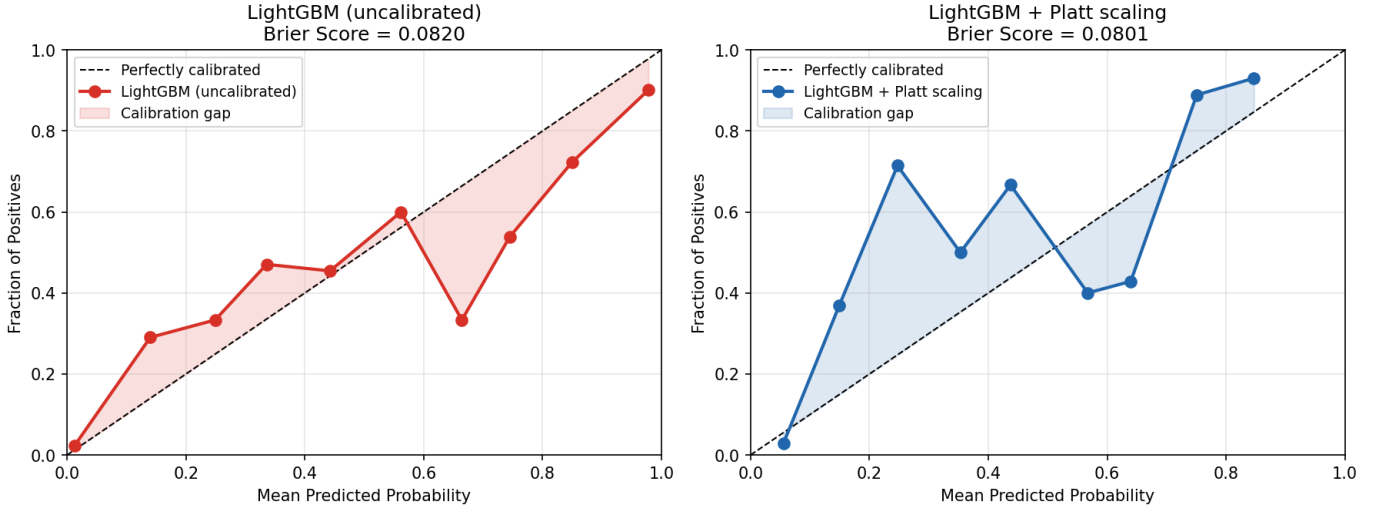


Fig. 6. Probability calibration analysis. Left: uncalibrated LightGBM (Brier = 0.082). Right: after Platt scaling (Brier = 0.080). Closer alignment to the diagonal indicates better-calibrated maintenance probabilities, which is critical for setting alert thresholds in safety-sensitive deployment contexts.

TABLE VII
SERVICE TIME REGRESSION RESULTS — SYNTHETIC DATASET
(LIGHTGBM BEST)

Model	RMSE (days)	MAE (days)	R^2
Random Forest	6.20	2.48	0.9940
XGBoost	6.00	2.45	0.9944
LightGBM (best)	5.71	2.33	0.9949

Target range: 0–365 days. Time-aware 70/30 split on synthetic dataset ($n=1,500$). R^2 reflects simulation-domain performance only; real-world generalisation is not implied.

is a substantially harder problem due to driver heterogeneity, vehicle aging effects not captured in the degradation model, and component interactions outside the simulation scope. Field validation is required before these regression metrics can inform deployment decisions.

VII. LIMITATIONS AND FUTURE WORK

Several limitations should be acknowledged explicitly. First, the physics-informed synthetic dataset, while designed with probabilistic labels and additive feature contributions, has not been validated against physical component teardown data. Degradation model parameters are drawn from published engineering literature, but actual in-service degradation is subject to manufacturing variability, maintenance history interactions, and usage patterns outside the simulation scope. Field validation on instrumented vehicles is a necessary prerequisite for deployment.

Second, the AI4I 2020 benchmark, while real-world, models industrial milling machine failures rather than automotive component failures. The feature set—air temperature, rotational speed, torque, and tool wear—has different physical characteristics to automotive brake, tire, and battery degradation. This work uses AI4I to validate the algorithmic pipeline’s ability to generalise to real failure data; whether that pipeline

performs similarly on automotive-specific field data remains an open empirical question.

Third, the edge latency measurements are modelled from LTE round-trip time estimates and local inference benchmarks rather than measured on deployed hardware in a moving vehicle. Network conditions, sensor update rates, and competing compute workloads in a real vehicle will affect observed latency and should be characterised in field trials.

Fourth, the calibration improvement from Platt scaling is modest (Brier score 0.082 \rightarrow 0.080). The calibration curves exhibit irregular patterns consistent with insufficient test set size for calibration fitting. Isotonic regression or temperature scaling on a larger held-out set may yield more substantial improvements.

Future work will focus on: (i) field deployment on an instrumented vehicle fleet to collect ground-truth maintenance labels under real-world conditions; (ii) integration of the AI4I pipeline with domain adaptation techniques to transfer learned representations to automotive sensor distributions; (iii) federated learning to enable privacy-preserving model improvement across fleet vehicles; and (iv) formal security and privacy evaluation of the DMS integration.

VIII. CONCLUSION

This paper presented a contextually-aware predictive maintenance framework for connected vehicles, evaluated across three complementary experimental layers designed to address common shortcomings of prior work in this space. The ablation study provides the first causal evidence—to the authors’ knowledge—that V2X-sourced contextual features contribute meaningfully to automotive maintenance prediction: removing environmental features reduces macro F1 by 0.026, and operating on internal mechanical features alone produces a 0.049-point deficit versus the full contextual model. SHAP analysis confirms that four contextual and interaction features appear

Experiment 7: Service Time Regression — LightGBM

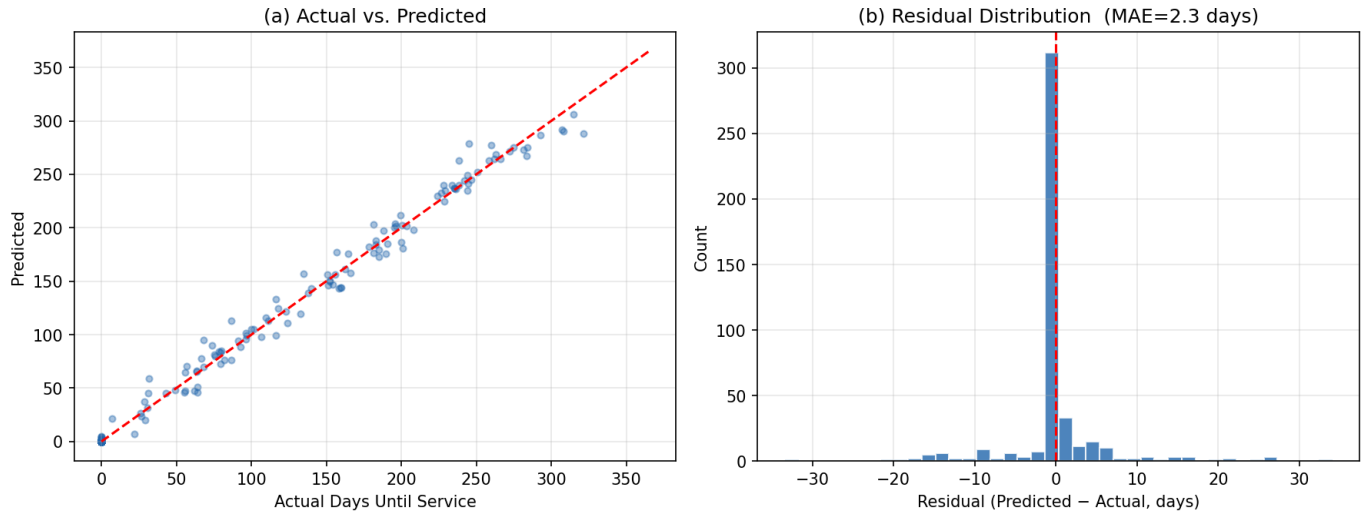


Fig. 7. Service time regression — LightGBM. (a) Actual vs. predicted days until service; near-diagonal scatter indicates high accuracy within the simulation. (b) Residual distribution; median residual ≈ 0 , IQR $\approx \pm 3$ days. Note: R^2 of 0.9949 reflects simulation-domain performance and should not be interpreted as real-world generalisation.

in the top nine predictors, with directional effects consistent with physical degradation mechanisms.

The AI4I 2020 benchmark evaluation demonstrates that the LightGBM classification pipeline generalises to real industrial failure data, achieving AUC-ROC of 0.973 under rigorous 5-fold cross-validation. The noise sensitivity analysis empirically characterises the performance-noise tradeoff, showing F1 remains above 0.879 under low-to-moderate noise and degrading predictably at higher noise levels—providing an evidence-based foundation for real-world performance expectations. Edge-based inference reduces estimated response latency from 3.5 seconds to under 1.0 second relative to cloud-only processing, based on modelled benchmarks derived from published LTE round-trip time characterisations and local TFLite INT8 inference benchmarks on comparable edge hardware. These are modelled estimates; field measurement on deployed hardware in a moving vehicle is required to confirm these figures, as noted in Section VII.

Taken together, these results establish a rigorous, reproducible proof-of-concept for the proposed architecture and identify a clear experimental roadmap: field deployment on instrumented vehicles to obtain automotive ground-truth failure labels, domain adaptation to bridge the industrial-to-automotive gap demonstrated by the AI4I experiments, and federated fleet learning for privacy-preserving continuous improvement. All code and the synthetic dataset generation pipeline are publicly available to support further research.

DECLARATIONS

Funding The authors received no specific funding for this research.

Conflicts of Interest The authors declare that they have no conflicts of interest.

Ethics Approval Not applicable. This study does not involve human participants, animals, or sensitive personal data.

Consent to Participate Not applicable.

Consent for Publication Not applicable.

Data Availability The study utilizes the publicly available AI4I 2020 Predictive Maintenance Dataset from the UCI Machine Learning Repository. The dataset can be accessed at: <https://archive.ics.uci.edu/dataset/601/ai4i+2020+predictive+maintenance+dataset>

Code Availability All source code, implementation scripts, and supplementary materials used in this study are publicly available at: <https://github.com/Kushalk0677/AI-Driven-Predictive-Maintenance-with-Real-Time-Contextual-Data-Fusion-for-Connected-Vehicles>

Author Contributions Kushal Khemani conceived the research idea, developed the methodology, implemented the models, conducted the experiments, and drafted the manuscript. Dr. Anjum Nazir Qureshi provided academic supervision, technical guidance, and critical revisions of the manuscript.

Acknowledgements The authors would like to acknowledge the UCI Machine Learning Repository for providing the AI4I 2020 Predictive Maintenance Dataset used in this research.

REFERENCES

- [1] A. K. S. Jardine, D. Lin, and D. Banjevic, “A review on machinery diagnostics and prognostics implementing condition-based maintenance,” *Mech. Syst. Signal Process.*, vol. 20, no. 7, pp. 1483–1510, 2006. <https://doi.org/10.1016/j.ymsp.2005.09.012>
- [2] R. K. Mobley, *An Introduction to Predictive Maintenance*, 2nd ed. Oxford: Butterworth-Heinemann, 2002.
- [3] T. P. Carvalho *et al.*, “A systematic literature review of machine learning methods applied to predictive maintenance,” *Comput. Ind. Eng.*, vol. 137, p. 106024, 2019. <https://doi.org/10.1016/j.cie.2019.106024>

- [4] H. M. Hashemian, "State-of-the-art predictive maintenance techniques," *IEEE Trans. Instrum. Meas.*, vol. 60, no. 1, pp. 226–236, 2011. <https://doi.org/10.1109/TIM.2010.2047662>
- [5] J. Lee, F. Wu, W. Zhao, M. Ghaffari, L. Liao, and D. Siegel, "Prognostics and health management design for rotary machinery systems," *Mech. Syst. Signal Process.*, vol. 42, no. 1–2, pp. 314–334, 2014. <https://doi.org/10.1016/j.ymssp.2013.06.035>
- [6] T. Wuest, D. Weimer, C. Irgens, and K. D. Thoben, "Machine learning in manufacturing: Advantages, challenges, and applications," *Prod. Manuf. Res.*, vol. 4, no. 1, pp. 23–45, 2016.
- [7] G. A. Susto, A. Schirru, S. Pampuri, S. McLoone, and A. Beghi, "Machine learning for predictive maintenance: A multiple classifier approach," *IEEE Trans. Ind. Inform.*, vol. 11, no. 3, pp. 812–820, 2015. <https://doi.org/10.1109/TII.2014.2349359>
- [8] S. Matzka, "Explainable artificial intelligence for predictive maintenance applications," in *Proc. 3rd Int. Conf. Artif. Intell. Ind. (AI4I 2020)*, 2020. UCI ML Repository. <https://archive.ics.uci.edu/dataset/601/>
- [9] S. Ferreira, A. Arnaiz, B. Sierra, and I. Irigoien, "Ensemble approach for automotive predictive maintenance," *IEEE Access*, vol. 8, pp. 180507–180518, 2020. <https://doi.org/10.1109/ACCESS.2020.3031394>
- [10] W. Zhang, D. Yang, and H. Wang, "Data-driven methods for predictive maintenance of industrial equipment: A survey," *IEEE Syst. J.*, vol. 13, no. 3, pp. 2213–2227, 2022. <https://doi.org/10.1109/JSYST.2018.2813800>
- [11] A. Gupta and M. S. Raval, "A review of machine learning techniques for automotive maintenance prediction," *Int. J. Eng. Res. Technol.*, vol. 5, no. 10, pp. 111–117, 2016.
- [12] B. Khaleghi, A. Khamis, F. O. Karray, and S. N. Razavi, "Multisensor data fusion: A review of the state-of-the-art," *Inf. Fusion*, vol. 14, no. 1, pp. 28–44, 2013. <https://doi.org/10.1016/j.inffus.2011.08.001>
- [13] D. L. Hall and J. Llinas, "An introduction to multisensor data fusion," *Proc. IEEE*, vol. 85, no. 1, pp. 6–23, 1997. <https://doi.org/10.1109/5.554205>
- [14] J. B. Kenney, "Dedicated short-range communications (DSRC) standards in the United States," *Proc. IEEE*, vol. 99, no. 7, pp. 1162–1182, 2011. <https://doi.org/10.1109/JPROC.2011.2132790>
- [15] H. Seo *et al.*, "LTE evolution for V2X services," *IEEE Commun. Mag.*, vol. 54, no. 6, pp. 22–28, 2016. <https://doi.org/10.1109/MCOM.2016.7452272>
- [16] W. Shi, J. Cao, Q. Zhang, Y. Li, and L. Xu, "Edge computing: Vision and challenges," *IEEE Internet Things J.*, vol. 3, no. 5, pp. 637–646, 2016. <https://doi.org/10.1109/JIOT.2016.2579198>
- [17] W. Yu *et al.*, "A survey on the edge computing for the Internet of Things," *IEEE Access*, vol. 6, pp. 6900–6919, 2017. <https://doi.org/10.1109/ACCESS.2017.2778504>
- [18] J. Chen, X. Ran, and X. Ma, "Deep learning with edge computing: A review," *Proc. IEEE*, vol. 107, no. 8, pp. 1655–1674, 2019. <https://doi.org/10.1109/JPROC.2019.2921977>
- [19] N. D. Lane *et al.*, "DeepX: A software accelerator for low-power deep learning inference on mobile devices," in *Proc. ACM/IEEE IPSN*, 2016.
- [20] G. Ke *et al.*, "LightGBM: A highly efficient gradient boosting decision tree," in *Adv. Neural Inf. Process. Syst.*, vol. 30, 2017. https://papers.nips.cc/paper_files/paper/2017/hash/6449f44a102fde848669bdd9eb6b76fa-Abstract.html
- [21] G. Vachtsevanos, F. Lewis, M. Roemer, A. Hess, and B. Wu, *Intelligent Fault Diagnosis and Prognosis for Engineering Systems*. Hoboken, NJ: Wiley, 2006.
- [22] J. Bokrantz, A. Skoogh, C. Berlin, and J. Stahre, "Maintenance in digitalised manufacturing: Delphi-based scenarios for 2030," *Int. J. Prod. Econ.*, vol. 191, pp. 154–169, 2017. <https://doi.org/10.1016/j.ijpe.2017.06.012>
- [23] L. Swanson, "Linking maintenance strategies to performance," *Int. J. Prod. Econ.*, vol. 70, no. 3, pp. 237–244, 2001. [https://doi.org/10.1016/S0925-5273\(00\)00128-8](https://doi.org/10.1016/S0925-5273(00)00128-8)
- [24] H. Hartenstein and K. Laberteaux, "A tutorial survey on vehicular ad hoc networks," *IEEE Commun. Mag.*, vol. 46, no. 6, pp. 164–171, 2008. <https://doi.org/10.1109/MCOM.2008.4539481>
- [25] X. S. Si, W. Wang, C. H. Hu, and D. H. Zhou, "Remaining useful life estimation — A review on the statistical data driven approaches," *Eur. J. Oper. Res.*, vol. 213, no. 1, pp. 1–14, 2011. <https://doi.org/10.1016/j.ejor.2011.02.021>
- [26] I. Goodfellow, Y. Bengio, and A. Courville, *Deep Learning*. Cambridge, MA: MIT Press, 2016. <https://www.deeplearningbook.org/>
- [27] T. Hastie, R. Tibshirani, and J. Friedman, *The Elements of Statistical Learning*, 2nd ed. New York, NY: Springer, 2009. <https://hastie.su.domains/ElemStatLearn/>
- [28] S. I. Nikolenko, *Synthetic Data for Deep Learning*. Cham: Springer, 2021.
- [29] A. Talebpour and H. S. Mahmassani, "Influence of connected and autonomous vehicles on traffic flow stability," *Transp. Res. C Emerg. Technol.*, vol. 71, pp. 143–163, 2016. <https://doi.org/10.1016/j.trc.2016.07.009>
- [30] F. Provost and T. Fawcett, *Data Science for Business*. Sebastopol, CA: O'Reilly Media, 2013.
- [31] N. V. Chawla, K. W. Bowyer, L. O. Hall, and W. P. Kegelmeyer, "SMOTE: Synthetic minority over-sampling technique," *J. Artif. Intell. Res.*, vol. 16, pp. 321–357, 2002. <https://doi.org/10.1613/jair.953>
- [32] S. M. Lundberg and S.-I. Lee, "A unified approach to interpreting model predictions," in *Adv. Neural Inf. Process. Syst.*, vol. 30, 2017. <https://proceedings.neurips.cc/paper/2017/hash/8a20a8621978632d76c43dfd28b67767-Abstract.html>
- [33] J. C. Platt, "Probabilistic outputs for support vector machines and comparisons to regularized likelihood methods," in *Advances in Large Margin Classifiers*, A. Smola, P. Bartlett, B. Schölkopf, and D. Schuurmans, Eds. Cambridge, MA: MIT Press, 1999, pp. 61–74.